Modeling and Aggregating DER Flexibility Region in VPPs
An Elimination and Projection Approach

Li, Chuyi; Zheng, Kedi; Feng, Cheng; Chen, Qixin; Vergara, Pedro P.

DOI
10.1109/PESGM51994.2024.10688569

Publication date
2024

Document Version
Final published version

Published in
2024 IEEE Power and Energy Society General Meeting, PESGM 2024

Modeling and Aggregating DER Flexibility Region in VPPs: An Elimination and Projection Approach

Chuyi Li, Kedi Zheng, Cheng Feng, Qixin Chen*
Department of Electrical Engineering
Tsinghua University, Beijing, China 100084
qxchen@tsinghua.edu.cn

Pedro P. Vergara
Department of Electrical Sustainable Energy
Delft University of Technology, 2628 CD Delft, Netherlands

2024 IEEE Power & Energy Society General Meeting (PESGM) | 979-8-3503-8183-2/24/$31.00 ©2024 IEEE | DOI: 10.1109/PESGM51994.2024.10688569

***Abstract*—The power generation and consumption of distributed energy resources (DERs) offer significant flexibility potential, which can be utilized to provide services such as peak and frequency regulation. DERs introduce a vast number of variables and constraints, making it complicated to directly integrate them into upper-level dispatch. To address this challenge, virtual power plants (VPPs) emerge, which treat diverse DERs as a collective entity and use aggregated flexibility envelopes to reduce the variable and constraint scale, facilitating upper-level optimization. In VPPs, unified DER modeling and efficient DER aggregation play a crucial role but are challenging. This paper first introduces a novel unified polytope model to represent heterogenous DERs' flexibility region. A coordination transformation is utilized to eliminate redundant variable dimensions and maintain DERs' interface characteristics. A sample-based projection method is then developed, further removing all state variables, resulting in a unified flexibility region. This method is then utilized to calculate the Minkowski sums of individual flexibility polytopes for aggregation. The results of numerical tests demonstrate a considerable reduction in computation time and maintain satisfactory accuracy when the proposed modeling and aggregation approach is adopted.**

***Index Terms*—Virtual power plant, distributed energy resources, polytope, load aggregation.**

I. Introduction

The rise in the penetration rate of renewable energy poses significant challenges to the operation of the system, highlighting the shortage of flexibility. Meanwhile, the massive amount of distributed energy resources (DERs) has come into the horizon and has tremendous flexibility potential. In traditional system operation, electricity demand is considered rigid and must be balanced in real-time by generators. However, many electricity demands have a certain flexibility, which can work together to provide multiple services such as peak and frequency regulation. These flexible resources are often small-scale, distributed, and heterogeneous. A typical distribution system may access up to 10^6 DERs [1], making their management difficult. Virtual power plants (VPPs) provide a practical approach to managing DERs as a whole to interact with the power grid [2]. The core of the VPP lies in the unified modeling and efficient aggregating of heterogeneous DERs.

This work was supported by the International (NSFC-NWO) Joint Research Project of National Natural Science Foundation of China under Grant 52161135201, the National Natural Science Foundation of China under Grant 52307103, and the Major Smart Grid Joint Project of the National Natural Science Foundation of China and State Grid under Grant U2066205.

For DER modeling, it includes a large variety of resources, such as distributed generators (DGs) and energy storage systems (ESSs). Traditionally, the models of these resources are established based on their operational characteristics. However, directly establishing these models results in highly heterogeneous mathematical forms that are difficult to aggregate. Therefore, one focus of research lies in how to develop unified models. Barot et al. first introduced polytope modeling [1]. They take the flexibility model described by a set of linear inequalities as a polytope in a high-dimensional space and unify heterogeneous polytopes into the interface variable space. This polytope modeling method has since been widely applied [3], [4], [5]. However, in these studies, input and output power are separately treated, and equality constraints are directly converted into inequalities. These practices significantly increase the dimensionality of the resulting polytope and hinder its integration into higher-level network optimization.

For DER aggregation, including all DERs' constraints directly into the upper-level optimization would result in an excessively large problem that cannot be efficiently solved. Therefore, aggregation has become another widely studied problem. The mathematical essence of aggregating polytopes is the Minkowski sum of sets. However, for polytopes represented by the intersection of half-spaces (H-representation), solving the Minkowski sum exactly requires vertex enumeration, which is NP-hard [6]. Barot et al. proposed a relaxed algorithm for aggregation and proved that it provided an outer approximation of the exact result [1]. Outer approximation tends to be over-optimistic in estimating the flexibility of the VPP. Therefore, subsequent research proposed a series of conservative inner approximation algorithms, such as box [7], ellipse [8], and zonotope approximation [3]. However, these methods pre-assumed the shape of the aggregated polytope in advance, which can accumulate significant errors in high dimensions.

Against the background, this paper proposes a novel unified polytope modeling and aggregation approach. For the modeling of DERs, net power instead of separate input and output power is adopted as interface variables, and a coordinate transformation method to handle variable redundancy caused by equality constraints is also introduced, significantly reducing the dimension of the polytope and making the model easier

979-8-3503-1637-7/24/$31.00 ©2024 IEEE

to be embedded in higher-level optimization problems. For DER aggregation, the Minkowski sum of polytope aggregation is transformed into a projection problem. By combining the proposed coordinate transformation method and the Monte Carlo (MC) method, an approximation of the aggregated result is obtained, avoiding error accumulation caused by pre-assumed shapes.

II. Polytope Modeling of DERs

A DER is usually modeled via linear constraints concerning its state variables. The constraints can be given by its corresponding difference state equations and upper/lower bounds. This is naturally a polytope of H-representation:

$$\left\{ \begin{bmatrix} \boldsymbol{X}^{\text{inner}} \\ \boldsymbol{X}^{\text{IF}} \end{bmatrix} \middle| \begin{bmatrix} \boldsymbol{A}^{\text{inner}} \boldsymbol{A}^{\text{IF}} \end{bmatrix} \begin{bmatrix} \boldsymbol{X}^{\text{inner}} \\ \boldsymbol{X}^{\text{IF}} \end{bmatrix} \leq \boldsymbol{b} \right\} \tag{1}$$

where $\boldsymbol{A}$, $\boldsymbol{b}$, and $\boldsymbol{X}$ represent the coefficient matrix, the right-hand side vector, and the variable vector; the superscript IF and inner correspond to DER's interface and inner state variables, respectively. The two-tuple $\left(\begin{bmatrix} \boldsymbol{A}^{\text{inner}} \boldsymbol{A}^{\text{IF}} \end{bmatrix}, \boldsymbol{b} \right)$ is chosen to uniquely represent this polytope.

Heterogeneous DERs correspond to different state equations and bound constraints, resulting in polytopes in different geometric spaces. A projection process is adopted to unify them in the interface variable space:

$$(1) \overset{\text{Project}}{\Longrightarrow} \left\{ \boldsymbol{X}^{\text{IF}} \middle| \boldsymbol{\Pi}^{\text{IF}} \boldsymbol{X}^{\text{IF}} \leq \boldsymbol{\pi}^{\text{IF}} \right\} \tag{2}$$

The two-tuple $\left(\boldsymbol{\Pi}^{\text{IF}}, \boldsymbol{\pi}^{\text{IF}} \right)$ represents the polytope in the unified space and is given through projection to the interface.

In the following subsections, DGs and ESSs are given as examples to illustrate this modeling and projection process.

A. DERs Without State Variables

Some DERs have no inner state variables and only one operating variable, the output power, such as DGs. Considering the power limit and ramping limit, DG can be modeled as follows:

$$\underline{P}^{\text{DG}} \leq P_t^{\text{DG}} \leq \overline{P}^{\text{DG}} \tag{3a}$$

$$-\underline{\delta}^{\text{DG}} \leq P_{t-1}^{\text{DG}} - P_t^{\text{DG}} \leq \overline{\delta}^{\text{DG}} \tag{3b}$$

where P is the interface output power; δ is the ramping rate; overline and underline represent the upper and lower boundaries; t is the time index.

Polytope described by (3) does not have inner state variables. Thus, it can be naturally transformed into a polytope in the interface space, represented as $\left(\boldsymbol{\Pi}^{\text{DG}}, \boldsymbol{\pi}^{\text{DG}} \right)$.

B. DERs With State Variables

Some DERs are more complicated, such as ESSs, which have an inner state variable state-of-charge (SOC). ESSs also have two operation modes: charging and discharging. These variables must be eliminated when projecting to the interface space. ESS can be modeled as follows [9]:

$$P_t^{\text{ESS}} = P_t^{\text{ESS,out}} - P_t^{\text{ESS,in}} \tag{4a}$$

$$\underline{P}^{\text{ESS,in/out}} \leq P_t^{\text{ESS,in/out}} \leq \overline{P}^{\text{ESS,in/out}} \tag{4b}$$

$$-\underline{\delta}^{\text{ESS,in/out}} \leq P_{t-1}^{\text{ESS,in/out}} - P_t^{\text{ESS,in/out}} \leq \overline{\delta}^{\text{ESS,in/out}} \tag{4c}$$

$$E_t^{\text{ESS}} = \eta^{\text{ESS}} E_{t-1}^{\text{ESS}} + \Delta T \left(\alpha^{\text{ESS,in}} P_t^{\text{ESS,in}} - \alpha^{\text{ESS,out}} P_t^{\text{ESS,out}} \right) \tag{4d}$$

$$\underline{E}^{\text{ESS}} \leq E_t^{\text{ESS}}(t) \leq \overline{E}^{\text{ESS}} \tag{4e}$$

where P, E, and δ are the interface power, the residual energy, and the ramping rate; η and α represent the efficiencies of charging and discharging power; overline and underline represent the upper and lower boundaries; superscript in and out stand for charging and discharging operation mode of the ESS, respectively; ΔT is the time interval; t is the time index.

Since model (4) has two operation modes and inner state variables $E_{n,t}^{\text{ESS}}$, one possible method is to replace each equality with two opposite inequalities and take (4) directly as a high-dimensional polytope and then apply a projection algorithm. This results in more facets and dimensions of the original polytope. Unfortunately, accurate projection algorithms, such as Fourier–Motzkin Elimination (FME), have a double exponential time complexity of $O((n/4)^{2^d})$, where n and d represent the number of facets and the dimensions in which the projection is reduced. In high-dimensional cases, reducing the number of facets and dimensions of the original polytope is the priority. To improve efficiency, a coordinate transformation method is proposed to treat equalities separately. Rewrite (4) in compact form:

$$\boldsymbol{A}_1^{\text{ieq}} \begin{bmatrix} \boldsymbol{P}^{\text{in}} \\ \boldsymbol{P}^{\text{out}} \end{bmatrix} \leq \boldsymbol{b}_1^{\text{ieq}} \tag{5a}$$

$$\boldsymbol{A}_2^{\text{ieq}} \boldsymbol{E} \leq \boldsymbol{b}_2^{\text{ieq}} \tag{5b}$$

$$\begin{bmatrix} \boldsymbol{A}_1^{\text{eq}} & \boldsymbol{A}_2^{\text{eq}} \end{bmatrix} \left[\begin{array}{c} \boldsymbol{E} \\ \hline \boldsymbol{P}^{\text{in}} \\ \boldsymbol{P}^{\text{out}} \end{array} \right] = \boldsymbol{0} \tag{5c}$$

$$\begin{bmatrix} \boldsymbol{I} & -\boldsymbol{I} & \boldsymbol{I} \end{bmatrix} \left[\begin{array}{c} \boldsymbol{P}^{\text{in}} \\ \boldsymbol{P}^{\text{out}} \\ \hline \boldsymbol{P} \end{array} \right] = \boldsymbol{0} \tag{5d}$$

For (5c), $\begin{bmatrix} \boldsymbol{A}_1^{\text{eq}} & \boldsymbol{A}_2^{\text{eq}} \end{bmatrix}$ has full row rank, and:

$$(5c) \Leftrightarrow \boldsymbol{E} = -\left(\boldsymbol{A}_1^{\text{eq}}\right)^{-1} \boldsymbol{A}_2^{\text{eq}} \begin{bmatrix} \boldsymbol{P}^{\text{in}} \\ \boldsymbol{P}^{\text{out}} \end{bmatrix} \tag{6}$$

Substitute (6) into (5b) to eliminate $\boldsymbol{E}$:

$$-\boldsymbol{A}_2^{\text{ieq}} \left(\boldsymbol{A}_1^{\text{eq}}\right)^{-1} \boldsymbol{A}_2^{\text{eq}} \begin{bmatrix} \boldsymbol{P}^{\text{in}} \\ \boldsymbol{P}^{\text{out}} \end{bmatrix} \leq \boldsymbol{b}_2^{\text{ieq}} \tag{7}$$

Similarly, we want to eliminate inner state variables $\boldsymbol{P}^{\text{in}}$ and $\boldsymbol{P}^{\text{out}}$ using equality (5d). However, $\begin{bmatrix} \boldsymbol{I} & -\boldsymbol{I} \end{bmatrix}$ is not invertible. To perform elimination, we propose the following proposition:

Proposition 1. *For the following two regions:*

$$\Omega_1 = \left\{ \boldsymbol{y} \middle| \begin{array}{c} \begin{bmatrix} \boldsymbol{A}^{\text{eq}} & \boldsymbol{I} \end{bmatrix} \begin{bmatrix} \boldsymbol{x} \\ \boldsymbol{y} \end{bmatrix} = \boldsymbol{b}^{\text{eq}} \\ \boldsymbol{A}^{\text{ieq}} \boldsymbol{x} \leq \boldsymbol{b}^{\text{ieq}} \end{array} \right\}$$

and

$$\Omega_2 = \left\{ \boldsymbol{y} \middle| \boldsymbol{A}^{\mathrm{ieq}} \boldsymbol{T}^{-1} \begin{bmatrix} \boldsymbol{x}' \\ \boldsymbol{y} \end{bmatrix} \leq \boldsymbol{b}^{\mathrm{ieq}} + \boldsymbol{A}^{\mathrm{ieq}} \boldsymbol{T}^{-1} \begin{bmatrix} \boldsymbol{0} \\ \boldsymbol{b}^{\mathrm{eq}} \end{bmatrix} \right\}$$

where $\boldsymbol{A}^{\mathrm{eq}}$ *has full row rank;* $\boldsymbol{T}$ *is a maximal linearly independent group of* $\begin{bmatrix} \boldsymbol{I} \\ -\boldsymbol{A}^{\mathrm{eq}} \end{bmatrix}$ *that contains* $-\boldsymbol{A}^{\mathrm{eq}}$*;* $\begin{bmatrix} \boldsymbol{x}' \\ \boldsymbol{y} \end{bmatrix}$ *is the reduced state variables. The following holds:*

$$\Omega_1 = \Omega_2,$$

$$\dim(\boldsymbol{x}) - \dim(\boldsymbol{x}') = \mathrm{rank}(\boldsymbol{A}^{\mathrm{eq}})$$

The proof of this proposition is given in Appendix A.

Considering that region (5) has been reformed as constrained by (5a), (7), and (5d), which has the form expressed by **Propositon 1**. Thus, the region described by (5) equals to:

$$\begin{bmatrix} \boldsymbol{A}_1^{\mathrm{ieq}} \\ -\boldsymbol{A}_2^{\mathrm{ieq}} \left(\boldsymbol{A}_1^{\mathrm{eq}}\right)^{-1} \boldsymbol{A}_2^{\mathrm{eq}} \end{bmatrix} \boldsymbol{T}^{-1} \begin{bmatrix} \boldsymbol{x}' \\ \boldsymbol{P} \end{bmatrix} \leq \begin{bmatrix} \boldsymbol{b}_1^{\mathrm{ieq}} \\ \boldsymbol{b}_2^{\mathrm{ieq}} \end{bmatrix} \tag{8}$$

where $\boldsymbol{T}$ can be obtained as described in Appendix A. The equalities in the original model (4) are thus eliminated, and the corresponding polytope is transformed into a lower-dimensional one (reduces $\mathrm{rank}(\boldsymbol{A}^{\mathrm{eq}})$ dimensions) with fewer facets (reduces $2 \cdot \mathrm{rank}(\boldsymbol{A}^{\mathrm{eq}})$ facets). To further obtain the polytope in interface variable space, inner variables $\boldsymbol{x}'$ must be eliminated through a projection process, which is further discussed in later sections. The ESS polytope in the unified space is represented as $\left(\boldsymbol{\Pi}^{\mathrm{ESS}}, \boldsymbol{\pi}^{\mathrm{ESS}}\right)$.

III. Aggregation and Projection Approach

A. Aggregation Method

As mentioned in Section I, the number of DERs can be substantial within a typical VPP. Each DER necessitates the definition and establishment of a series of variables and constraints to portray its flexibility. Aggregation serves as the approach to approximate the VPP as a whole by disregarding redundant and less critical model details while preserving essential information needed to reconstruct the overall flexibility. This approach effectively controls the variable and constraint scale to a manageable level.

In the previous section, a polytope modeling method that represents various DERs as polytopes in a unified space is introduced. Based on this formulation, aggregation becomes a Minkowski sum problem. For the subsequent two polytopes $(\boldsymbol{A}_1, \boldsymbol{b_1})$ and $(\boldsymbol{A}_2, \boldsymbol{b_2})$:

$$\Omega_1 = \{\boldsymbol{x_1} \,|\boldsymbol{A}_1 \boldsymbol{x_1} \leq \boldsymbol{b_1}\}, \Omega_2 = \{\boldsymbol{x_2} \,|\boldsymbol{A}_2 \boldsymbol{x_2} \leq \boldsymbol{b_2}\} \tag{9}$$

Their Minkowski sum is defined as:

$$\{\boldsymbol{x_3} \,|\boldsymbol{x_3} = \boldsymbol{x_1} + \boldsymbol{x_2}, \boldsymbol{x_1} \in \Omega_1, \boldsymbol{x_2} \in \Omega_2\} \tag{10}$$

Intuitively, the aggregated region (10) can also be equivalently represented by a two-tuple $(\boldsymbol{A}_3, \boldsymbol{b_3})$. However, precisely calculating this two-tuple can be quite challenging, especially in high-dimensional cases [1]. To address this problem, transform (10) as follows:

$$\left\{ \boldsymbol{x_3} \middle| \begin{array}{c} \begin{bmatrix} \boldsymbol{I} & \boldsymbol{I} & -\boldsymbol{I} \end{bmatrix} \begin{bmatrix} \boldsymbol{x_1} \\ \boldsymbol{x_2} \\ \boldsymbol{x_3} \end{bmatrix} = \boldsymbol{0} \\ \begin{bmatrix} \boldsymbol{A}_1 & \boldsymbol{0} \\ \boldsymbol{0} & \boldsymbol{A}_2 \end{bmatrix} \begin{bmatrix} \boldsymbol{x_1} \\ \boldsymbol{x_2} \end{bmatrix} \leq \begin{bmatrix} \boldsymbol{b_1} \\ \boldsymbol{b_2} \end{bmatrix} \end{array} \right\} \tag{11}$$

which has the form in **Propositon 1**. Thus (11) equals to:

$$\begin{bmatrix} \boldsymbol{A}_1 & \boldsymbol{0} \\ \boldsymbol{0} & \boldsymbol{A}_2 \end{bmatrix} \boldsymbol{T}^{-1} \begin{bmatrix} \boldsymbol{x}' \\ \boldsymbol{x_3} \end{bmatrix} \leq \begin{bmatrix} \boldsymbol{b_1} \\ \boldsymbol{b_2} \end{bmatrix} \tag{12}$$

Subsequently, the two-tuple that represents the aggregated region can be derived through a projection:

$$(12) \overset{\text{Project}}{\Longrightarrow} \boldsymbol{A}_3 \boldsymbol{x_3} \leq \boldsymbol{b_3} \tag{13}$$

B. Sample-based Projection Method

As discussed in Section II-B and Section III-A, both unifying diverse polytopes into a common space and aggregation necessitate a projection process. Despite efforts to minimize dimensionality and the number of constraints, the projection remains challenging due to its exponential time complexity.

Projecting a polytope of H-representation involves calculating its vertices from a set of hyperplanes, which can be a complex task. To address this challenge, an MC sampling method based on a hit-and-run algorithm is employed [10]. This method allows for the random sampling of points from a uniform distribution within the polytope, which can then be easily projected to the desired lower-dimensional space. The region in which these projected sample points are distributed serves as an approximation of the original polytope's projection.

However, quantifying this region requires calculating the convex hull of the projected point set, which can also be a challenging task. To simplify the problem, a set of hyperplanes with predefined normal vectors is utilized to encompass all points. In the case of a projected space with N dimensions, the normal vectors of these hyperplanes are provided as follows:

$$\boldsymbol{\Gamma} = \begin{bmatrix} \boldsymbol{G} & -\boldsymbol{G} \end{bmatrix} \tag{14}$$

where

$$\boldsymbol{G} = \begin{bmatrix} 1 & 1 & \dots & 1 & & & & & \\ & 1 & \dots & 1 & 1 & \dots & 1 & & \\ & & \ddots & \vdots & & \ddots & \vdots & \dots & \\ & & & 1 & & & 1 & & 1 \end{bmatrix} \in \mathbb{R}^{N \times \frac{(1+N)N}{2}} \tag{15}$$

The ith normal vector is denoted as $\boldsymbol{\Gamma}_i$. This set of hyperplanes is generated from the zonotope proposed in [3], which has been discussed to be well suited to approximate high-dimensional polytopes.

The intercepts of this set of hyperplanes are then determined by solving a series of linear programming problems:

$$\min_{\boldsymbol{\beta}} \mathbf{1}^{\top} \cdot \boldsymbol{\beta} \tag{16}$$

TABLE I
PARAMENTER SPECIFICATIONS OF DG AND ESS

	DG	ESS
$\underline{P}^{\text{in}}/\overline{P}^{\text{in}}$ (kW)	-	0 / 10
$\underline{P}^{\text{out}}/\overline{P}^{\text{out}}$ (kW)	5 / 10	0 / 10
$\underline{\delta}^{\text{in}}/\overline{\delta}^{\text{in}}$ (kW/h)	-	5 / 5
$\underline{\delta}^{\text{out}}/\overline{\delta}^{\text{out}}$ (kW/h)	3 / 3	5 / 5
$\underline{E}/\overline{E}$ (kWh)	-	0 / 20
$\eta/\alpha^{\text{in}}/\alpha^{\text{out}}$	-	0.9 / 0.9 / 1.11

$$\text{s.t.}: \boldsymbol{X}^{\text{Proj}} \cdot \boldsymbol{\Gamma}_i \leq \boldsymbol{\beta},\ i = 1, \ldots, N(N+1)$$

where $\boldsymbol{\beta}$ is the intercept vector; row vectors of $\boldsymbol{X}^{\text{Proj}}$ are the projected sample point coordinates. Linear programming (16) gives the smallest polytope containing all sampling points under the predefined facet orientation. Thus, the two-tuple $(\boldsymbol{\Gamma}^\top, \boldsymbol{\beta})$ is used as the approximated projection result.

IV. CASE STUDY

In this section, numerical tests are devised to evaluate the proposed modeling and aggregating approach. A 3-interval case is first considered. In this case, polytopes representing different DERs are 3-dimensional, making visual interpretation possible. Then, the analysis is extended to more time intervals to evaluate the high-dimensional performance. The algorithm proposed in [1] is adopted as a baseline for comparison, while the volume error rate (VER) and the F-score are chosen as metrics. Volumes are computed based on the Quickhull algorithm [11], offering a rough illustration of scenario coverage. F-score, treating the polytope as a classification boundary, provides a more precise evaluation. Note that our proposed method efficiently handles cases up to 24 dimensions, but both metrics rely on exact results, which can only be computed for dimensions lower than 6 [1].

In both cases, a DG and an ESS model are implemented with the parameters detailed in Table I, and their aggregation is computed. The time interval is chosen to be 1 hour. These models are implemented in MATLAB and executed on a computer with an Intel i5 CPU and 16 GB of memory.

A. Analysis of 3-interval Coupled Case

In Fig. 1, a DG polytope, an ESS polytopes derived using exact vertex enumeration, and an ESS polytope derived using the proposed approximate projection are visualized respectively. The DG polytope has fewer facets (12 facets), while the ESS polytope is more irregular (28 facets). This indicates that the coordinate transformation and projection process complicates the polytope. For the implementation of the proposed projection, 3000 points are sampled, as depicted in Fig. 1. The VER and F-score of the approximated polytope are 4.06% and 0.91, respectively. The number of facets is reduced to 12, with a 57.14% decrease, significantly reducing the problem

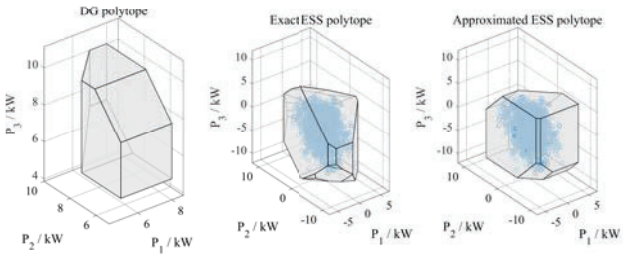

Fig. 1. Visualization of 3-interval coupled polytope modeling.

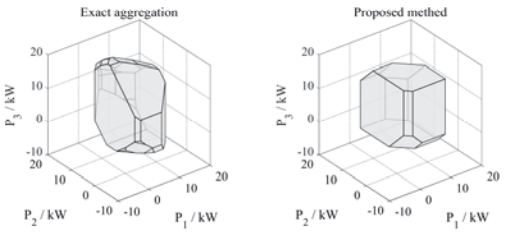

Fig. 2. Visualization of 3-interval coupled polytope aggregation.

TABLE II
ERROR EVALUATION

Dimensions		3	4	5
ESS Polytope	VER / %	4.06	0.78	8.99
	F-score	0.91	0.89	0.84
Aggregation (Method in [1])	VER / %	3.02	8.51	14.21
	F-score	0.86	0.80	0.72
Aggregation (Proposed)	VER / %	5.06	6.01	13.14
	F-score	0.84	0.81	0.75

scale. Fig. 2 provides a visualization of an exact aggregation, and an aggregation adopting the proposed method. These two polytopes have 39 and 12 facets, with a VER of 5.06% and an F-score of 0.84.

B. More Time Interval Coupled Cases

More coupled time intervals lead to polytopes in higher dimensions, exponentially complicating the calculation process. Table II summarizes the error evaluation of 3, 4, and 5 dimensions. The results indicate that as the dimension increases, a higher error is expected, and the proposed aggregation method outperforms the method in [1].

Fig. 3 compares the number of facets and computation time. As illustrated in the figure, the accurate methods, both in modeling and aggregation, encounter numerical challenges when addressing more than 5 coupled time intervals. In contrast, the proposed method exhibits a polynomial increase in the number of generated facets and the computation time as the number of coupled time intervals rises. More precisely, in the case of 5 coupled time intervals, when the VER for both the approximated modeling and the proposed aggregation

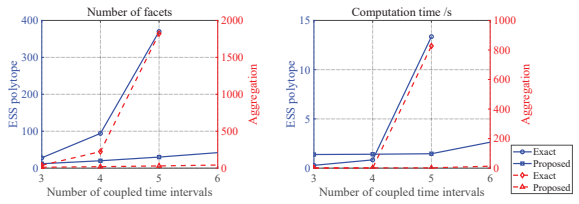

Fig. 3. Comparison of the number of facets and computation time.

methods are satisfactorily controlled under 15%, computation time are significantly reduced by 89.04% and 99.32%.

V. Conclusion

This paper introduces a unified modeling and aggregation method for characterizing the flexibility of DERs. DERs are first individually represented as diverse polytopes and subsequently mapped into a unified target space. These unified polytopes are then aggregated. A coordinate transform and a projection method are developed to facilitate the process. Numerical tests are conducted. The results illustrate that the proposed modeling and aggregation approach reduces computation time by 89.04% and 99.32% while controlling the VER under 15%. This confirms the effectiveness of the proposed approach. In future research, network constraints will be studied and integrated into the current approach, providing a more thorough characterization of the flexibility across the entire distribution system.

Appendix A
Proof of Proposition 1

Lemma 1. *The following two equalities are equivalent:*

$$\begin{bmatrix} \boldsymbol{A}^{\mathrm{eq}} & \boldsymbol{I} \end{bmatrix} \begin{bmatrix} \boldsymbol{x} \\ \boldsymbol{y} \end{bmatrix} = \boldsymbol{b}^{\mathrm{eq}} \tag{A.1a}$$

$$\Leftrightarrow \begin{bmatrix} \boldsymbol{x}' \\ \boldsymbol{y} \end{bmatrix} = \boldsymbol{T}\boldsymbol{x} + \begin{bmatrix} \boldsymbol{0} \\ \boldsymbol{b}^{\mathrm{eq}} \end{bmatrix} \tag{A.1b}$$

Proof. $\Rightarrow$: From (A.1a):

$$\begin{bmatrix} \boldsymbol{x} \\ \boldsymbol{y} \end{bmatrix} = \begin{bmatrix} \boldsymbol{x} \\ -\boldsymbol{A}^{\mathrm{eq}}\boldsymbol{x} + \boldsymbol{b}^{\mathrm{eq}} \end{bmatrix} = \begin{bmatrix} \boldsymbol{I} \\ -\boldsymbol{A}^{\mathrm{eq}} \end{bmatrix} \boldsymbol{x} + \begin{bmatrix} \boldsymbol{0} \\ \boldsymbol{b}^{\mathrm{eq}} \end{bmatrix}$$

Since matrix $\begin{bmatrix} \boldsymbol{I} \\ -\boldsymbol{A}^{\mathrm{eq}} \end{bmatrix}$ has full column rank, there exists a maximal linearly independent group among its row vector. Since $\boldsymbol{A}^{\mathrm{eq}}$ has full row rank, this group can be chosen to contain $-\boldsymbol{A}^{\mathrm{eq}}$, denoted as $\boldsymbol{T}$. Then:

$$\begin{bmatrix} \boldsymbol{x}' \\ \boldsymbol{y} \end{bmatrix} = \boldsymbol{T}\boldsymbol{x} + \begin{bmatrix} \boldsymbol{0} \\ \boldsymbol{b}^{\mathrm{eq}} \end{bmatrix}$$

$\boldsymbol{T}$ can be calculated through Gauss-Jordan Elimination.

$\Leftarrow$: Since $\boldsymbol{T}$ is a maximal linearly independent group that contains $-\boldsymbol{A}^{\mathrm{eq}}$, which can be denoted as:

$$\boldsymbol{T} = \begin{bmatrix} \dots & \boldsymbol{e}(k) & \dots & -(\boldsymbol{A}^{\mathrm{eq}})^{\top} \end{bmatrix}^{\top}$$

There exists a matrix $\boldsymbol{M}$ to linearly combine vectors that gives:

$$\boldsymbol{M}^{\top}\boldsymbol{T} = \begin{bmatrix} \boldsymbol{I} & -(\boldsymbol{A}^{\mathrm{eq}})^{\top} \end{bmatrix}^{\top}$$

where $\boldsymbol{M} = \begin{bmatrix} \boldsymbol{m}_{11} & \boldsymbol{0} \\ \boldsymbol{m}_{21} & \boldsymbol{I} \end{bmatrix}$. Thus from (A.1b):

$$\boldsymbol{M}^{\top} \begin{bmatrix} \boldsymbol{x}' \\ \boldsymbol{y} \end{bmatrix} = \begin{bmatrix} \boldsymbol{I} \\ -\boldsymbol{A}^{\mathrm{eq}} \end{bmatrix} \boldsymbol{x} + \boldsymbol{M}^{\top} \begin{bmatrix} \boldsymbol{0} \\ \boldsymbol{b}^{\mathrm{eq}} \end{bmatrix}$$

Extract lower blocks to get:

$$\boldsymbol{y} = -\boldsymbol{A}^{\mathrm{eq}}\boldsymbol{x} + \boldsymbol{b}^{\mathrm{eq}} \;\Leftrightarrow\; \text{(A.1a)}$$

□

According to **Lemma 1**:

$$\Omega_1 = \left\{ \boldsymbol{y} \;\middle|\; \begin{bmatrix} \boldsymbol{x}' \\ \boldsymbol{y} \end{bmatrix} = \boldsymbol{T}\boldsymbol{x} + \begin{bmatrix} \boldsymbol{0} \\ \boldsymbol{b}^{\mathrm{eq}} \end{bmatrix} \atop \boldsymbol{A}^{\mathrm{ieq}}\boldsymbol{x} \le \boldsymbol{b}^{\mathrm{ieq}} \right\}$$

Since $\boldsymbol{T}$ is inversible:

$$\begin{aligned} & \boldsymbol{A}^{\mathrm{ieq}}\boldsymbol{x} \le \boldsymbol{b}^{\mathrm{ieq}} \\ \Leftrightarrow\; & \boldsymbol{A}^{\mathrm{ieq}}\boldsymbol{T}^{-1}\left(\begin{bmatrix} \boldsymbol{x}' \\ \boldsymbol{y} \end{bmatrix} - \begin{bmatrix} \boldsymbol{0} \\ \boldsymbol{b}^{\mathrm{eq}} \end{bmatrix} \right) \le \boldsymbol{b}^{\mathrm{ieq}} \\ \Leftrightarrow\; & \boldsymbol{A}^{\mathrm{ieq}}\boldsymbol{T}^{-1} \begin{bmatrix} \boldsymbol{x}' \\ \boldsymbol{y} \end{bmatrix} \le \boldsymbol{b}^{\mathrm{ieq}} + \boldsymbol{A}^{\mathrm{ieq}}\boldsymbol{T}^{-1} \begin{bmatrix} \boldsymbol{0} \\ \boldsymbol{b}^{\mathrm{eq}} \end{bmatrix} \end{aligned}$$

Thus $\Omega_1 = \Omega_2$.

Meanwhile, also from **Lemma 1**:

$$\begin{aligned} & \mathrm{rank}(\boldsymbol{T}) = \dim(\boldsymbol{x}') + \dim(\boldsymbol{y}) = \dim(\boldsymbol{x}) \\ \Rightarrow\; & \dim(\boldsymbol{x}) - \dim(\boldsymbol{x}') = \dim(\boldsymbol{y}) = \mathrm{rank}(\boldsymbol{A}^{\mathrm{eq}}) \end{aligned}$$

References

[1] S. Barot and J. A. Taylor, "A concise, approximate representation of a collection of loads described by polytopes," *International Journal of Electrical Power & Energy Systems*, vol. 84, pp. 55–63, 2017.

[2] D. Koraki and K. Strunz, "Wind and solar power integration in electricity markets and distribution networks through service-centric virtual power plants," *IEEE Transactions on Power Systems*, vol. 33, no. 1, pp. 473–485, 2017.

[3] F. L. Müller, J. Szabó, O. Sundström, and J. Lygeros, "Aggregation and disaggregation of energetic flexibility from distributed energy resources," *IEEE Transactions on Smart Grid*, vol. 10, no. 2, pp. 1205–1214, 2017.

[4] Z. Yi, Y. Xu, W. Gu, L. Yang, and H. Sun, "Aggregate operation model for numerous small-capacity distributed energy resources considering uncertainty," *IEEE Transactions on Smart Grid*, vol. 12, no. 5, pp. 4208–4224, 2021.

[5] S. Wang and W. Wu, "Aggregate flexibility of virtual power plants with temporal coupling constraints," *IEEE Transactions on Smart Grid*, vol. 12, no. 6, pp. 5043–5051, 2021.

[6] L. Zhao, H. Hao, and W. Zhang, "Extracting flexibility of heterogeneous deferrable loads via polytopic projection approximation," in *2016 IEEE 55th Conference on Decision and Control (CDC)*. IEEE, 2016, pp. 6651–6656.

[7] X. Chen, E. Dall'Anese, C. Zhao, and N. Li, "Aggregate power flexibility in unbalanced distribution systems," *IEEE Transactions on Smart Grid*, vol. 11, no. 1, pp. 258–269, 2019.

[8] E. Polymeneas and S. Meliopoulos, "Aggregate modeling of distribution systems for multi-period opf," in *2016 Power Systems Computation Conference (PSCC)*. IEEE, 2016, pp. 1–8.

[9] Q. Li and V. Vittal, "Non-iterative enhanced sdp relaxations for optimal scheduling of distributed energy storage in distribution systems," *IEEE Transactions on Power Systems*, vol. 32, no. 3, pp. 1721–1732, 2016.

[10] D. E. Kaufman and R. L. Smith, "Direction choice for accelerated convergence in hit-and-run sampling," *Operations Research*, vol. 46, no. 1, pp. 84–95, 1998.

[11] C. B. Barber, D. P. Dobkin, and H. Huhdanpaa, "The quickhull algorithm for convex hulls," *ACM Transactions on Mathematical Software (TOMS)*, vol. 22, no. 4, pp. 469–483, 1996.